# Sky Savers: Leveraging Drone Technology for Victim Localization in Avalanche Rescue via Transceiver Signal Analysis

Robin Vetsch<sup>1,3</sup>•a, Samuel Kranz<sup>2</sup>•b, Tindaro Pittorino<sup>2</sup>•c, Peter de Baets<sup>4</sup>, Martial Châteauvieux<sup>4</sup>, Christoph Würsch<sup>3</sup>•d, Daniel Lenz<sup>3</sup> and Sebastien Gros<sup>1</sup>•e

Keywords: Avalanche Rescue, Victim Localization, Vertical Take-Off and Landing (VTOL) System, Avalanche

Transceiver.

Abstract: In modern avalanche rescues, the search for buried victims is carried out primarily using a state-of-the-art

handheld transceiver. However, in situations where the rescuers do not have the necessary experience, or if the victims are buried in areas that can be dangerous for the rescuers, e.g. due to the risk of secondary avalanches, this search process can be time-consuming, complex and dangerous. To overcome these challenges, we propose a proof-of-concept (PoC) of a search system based on an autonomous vertical take-off and landing (VTOL) aircraft that could significantly reduce search time, even in the case of multiple overlapping signal sources attributable to multiple victims or where conventional methods are not sufficiently efficient, e.g. in the case of large-scale avalanches. Electric drones or VTOL systems cannot be used because electro-magnetic interference (EMI) blocks the signal from the sending avalanche transceiver. By replacing electromagnetically noisy DC motors with a turbine, we effectively reduce electro-magnetic interference in the signal stream and demonstrate sub-meter localization accuracy under realistic field conditions. We employ a two-stage Extended Kalman Filter (EKF) approach to estimate the stationary target coordinates. Eventually, a VTOL system also allows for operations in adverse weather and rugged alpine terrain, greatly extending the

practical capability of search and rescue missions.

## 1 INTRODUCTION

On average, around 100 people die in avalanche accidents every winter in Europe (Association, 2025). This high number of fatalities motivates the development of an automated system to locate buried victims as quickly as possible.

In modern avalanche rescues, the search for buried victims is carried out primarily using commercially available handheld avalanche transceivers (Mammut, 2024b). The clinical study conducted by Brugger et al. (Brugger et al., 2007) showed how the use of an avalanche transceiver or an airbag could reduce

a https://orcid.org/0009-0007-8099-9457

<sup>b</sup> https://orcid.org/0009-0006-6766-6458

co https://orcid.org/0009-0005-7548-1130

dip https://orcid.org/0000-0002-1337-3477

e https://orcid.org/0000-0001-6054-2133

the probability of mortality. Rescuers rely on these transceivers to locate individuals by following the strength and direction of the signals, moving closer to the strongest signal to pinpoint the victim's location. Although this method can be effective, the rescuer must be proficient in using the device and interpreting the visualizations on the graphical user interface (GUI). In scenarios where rescuers have limited or no experience, or when there are multiple victims buried under the avalanche, the search process can become time consuming and complex, increasing the chance of deadly fatalities (Falk et al., 1994).

To address these challenges, we propose a VTOL search platform designed for fully automated operation, capable of drastically reducing victim localization times over vast avalanche terrains. With the combination of slow flight, vertical take-off and landing, and fast cruise flight to the accident site, our system

<sup>&</sup>lt;sup>1</sup>Department of Engineering Cybernetics, Norwegian University of Science and Technology, Høgskoleringen 1, Trondheim,

<sup>&</sup>lt;sup>2</sup>Institute for Electronics, Sensors and Actuators, Eastern Switzerland University of Applied Sciences, Werdenbergstrasse 4, Buchs, Switzerland

<sup>&</sup>lt;sup>3</sup>Institute for Computational Engineering, Eastern Switzerland University of Applied Sciences, Werdenbergstrasse 4, Buchs, Switzerland

<sup>&</sup>lt;sup>4</sup>ANAVIA, Bahnhofstrasse 37, Näfels, Switzerland

can reach confined and remote regions that are inaccessible to fixed-wing aircraft or ground vehicles, thus speeding up search operations in large areas.

As a sensor for localization, we used a commercially available *MAMMUT Barryvox Pulse* avalanche transceiver (Mammut, 2024a), which was integrated as an external payload onto the VTOL system. Our custom data analysis pipeline fuses the transceiver output with real-time GPS and heading information from the VTOL onboard navigation suite. As a backup, the sensor system also had a GPS module on board, which provided a data quality comparable to the GPS of the VTOL system. As input signals for the localization algorithm in this PoC, we used distance r and direction  $\varphi$  (in 15° increments) data of the transceiver device. This data is also available on the display of the device and is used today for mate searches by the user.

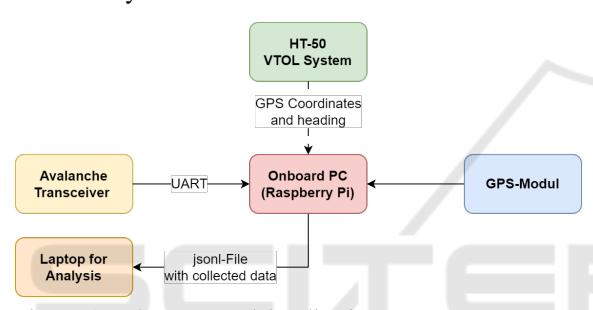


Figure 1: The proposed localization system (sensor system) consists of a 3-axis magnetic field sensor, an *MAM-MUT Barryvox Pulse* (yellow), an onboard computer for data collection (red) and a GPS module (blue). During flight, the VTOL system provides GPS and heading information which is used to compare the position estimations of the GPS module of the sensor system in blue.

# 1.1 Function of an Avalanche Transceiver

An avalanche transceiver essentially consists of an arrangement of three coils in the x, y and z directions, as shown in (Ayuso et al., 2015). The device can operate in two modes, send / transmit and search / receive. In send mode, the coil in the x direction, which has the highest sensitivity, and thanks to its size, generates a magnetic field. In search mode, the magnetic field emitted by the transmitter is coupled to the receiver via the x- and y-antennas and processed onboard. The z-antenna, which has the lowest sensitivity due to its limited length, is only used for the fine search. The fine search is defined as a specific search pattern (r < 5 m) that is used to locate the person out.

In send mode, the device sends a pulsed electromagnetic signal that is generated with an oscillation

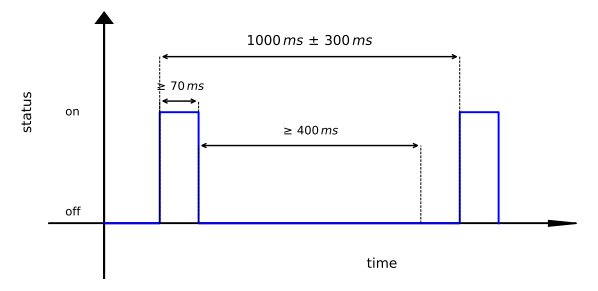


Figure 2: EN-normed pulse signal pattern including the minimal and maximal time length of the on- and off period. The pulse length and the off-time between two pulses is used for the separation of multiple targets.

frequency of  $f_s$  = 457 kHz and is approved worldwide for avalanche rescue. The signal is pulsed at regular intervals defined by the EN norm industry standard (ETSI, 2017), but with a unique repetition frequency to distinguish multiple signals when several transceivers transmit simultaneously. To minimize power consumption, the frequency of the signal is limited to approximately 1 Hz. The normed signal is shown in Figure 2.

# 1.2 Related Work

Recent research efforts in the development of automated systems for avalanche rescue have increasingly focused on the integration of sensor modalities into unmanned aerial vehicles (UAVs), such as drones for the rapid location of victims. However, commercial drones often exhibit significant drawbacks when operating in extreme environments, particularly with regard to electro-magnetic interference caused by conventional electric motors, which adversely impacts the performance of onboard avalanche transceivers. In addition, lithium batteries used in electric drones exhibit a loss of capacity in the cold winter weather, significantly limiting endurance.

A notable commercial initiative was the **Powder-Bee** system, a lightweight (600g) battery-powered drone designed for rapid search operations. **Powder-Bee** was engineered to autonomously execute predefined search patterns and land upon detection of a buried victim. Despite its innovative design, the company (Bluebird Mountain Inc.) was dissolved in 2021 and the EMI challenges inherent to its commercial platform remained unresolved (Bluebird, 2021).

Similarly, the **Alcedo** project from ETH Zurich represented an early student-driven effort to develop a foldable and easily transportable UAV for avalanche search and rescue. The system aimed to localize the buried victims according to the dimensions of the avalanche supplied by the user. However, the project did not progress beyond the prototype stages

due to robustness limitations and EMI issues (Alcedo, 2010).

The start-up **Nivitec** pursued an approach using a DJI Matrice 210 drone (DJI, 2025) equipped with an avalanche transceiver and a camera system. Their concept included plans for automated navigation to accident sites. However, the company stopped its activities in 2020, facing challenges related to limited flight endurance and operational speed (Nivitec, 2020).

An alternative mitigation strategy is employed by the **Atlas AVALANCHE PRO** system, which suspends the avalanche transceiver on a flexible pole 1 to 2 meters below the UAV to physically reduce EMI. Although this approach helps minimize interference, the uncontrolled orientation of the transceiver compromises the precision of the location, leading to the potential loss of critical positional data (ATLASUAS, 2025).

Beyond these commercial initiatives, a growing body of academic research has advanced UAV-based avalanche victim localization using transceiver systems. Silvagni et al. (Silvagni et al., 2017) developed a UAV system that integrates a commercial avalanche transceiver and thermal camera, demonstrating automated localization tested in Alpine conditions.

Azzollini et al. (Azzollini et al., 2020) proposed an extremum-seeking control strategy to autonomously steer a transceiver-equipped UAV toward the strongest signal, validated through simulation and hardware-in-the-loop tests.

The **AVERLA** project by Toson et al. (Toson et al., 2021) presented a custom high-gain antenna system for UAV-mounted transceiver tracking, achieving preliminary field success despite challenges in system miniaturization.

However, Janovec et al. (Janovec et al., 2022) reported severe EMI issues between UAV electronics and the beacon, concluding that conventional electric UAV platforms are ill suited for avalanche searches without extensive modifications. For the tests, they attached the avalanche transceiver with a 2m long rope underneath the drone.

Ricciardi (Ricciardi, 2017) showed that motorinduced EMI limits the sensitivity of avalanche transceivers to approximately 6 m with spinning propellers. EMI-grade aluminum shielding around the motors and arms extended reliable detection to approximately 7 m.

In contrast to these previous systems and research, our proposed VTOL-based solution offers several critical advances. Using a state-of-the-art avalanche transceiver integrated with real-time GPS and head-

ing data fusion, we substantially improve the robustness of the localization. Furthermore, the use of a robust, professional unmanned VTOL system powered by a turbine engine markedly reduces electromagnetic interference compared to electric motor platforms. This configuration enables high-speed automated operation in challenging and rough mountain environments, positioning our system as a significant step forward in UAV-based avalanche rescue technology in practice usage.

# 1.3 Methodology

The following subsections describe in detail the hardware setup of the payload, as well as the VTOL system setup and the localization algorithms.

## 1.3.1 Hardware Setup VTOL System

A VTOL system, a helicopter from ANAVIA, was used as a carrier system for the sensor system. ANAVIA's HT-50 helicopter (ANAVIA, 2025b) features a carbon fiber composite airframe and dual intermeshing Flettner rotors, emulating the full-scale flight dynamics of the larger HT-100 system (ANAVIA, 2025a). Its maximum take-off weight (MTOW) is 50 kg with a payload capacity of 20 kg. Power is provided by a 7 kW shaft-driven microturbine coupled to a high-performance gear. This type of drive is a major difference from all the other approaches and prototypes presented in 1.2.

Fuel is stored in a 17 L tank. The helicopter consumes approximately 10 L/h under cruise conditions. HT-50 achieves a maximum flight time of 90 min and has a top speed of 100 km/h. The system will be able to fly a pre-planned mission fully autonomously. However, the final version of the autopilot was not yet installed during the tests, so all flights were flown manually for our data collection.



Figure 3: HT-50 from ANAVIA was developed as a training platform for the larger HT-100. It has a payload of 20 kg, a flight time of 90 min and a maximum speed of 100 km/h.

#### 1.3.2 Hardware Setup Sensor System

Our system consists of an MAMMUT Pulse Barryvox avalanche transceiver, a Raspberry Pi, a GPS-module, an absolute Inertial Measurement Unit (IMU) and a Power Supply. The design and arrangement of the hardware components were chosen to achieve the best possible sensitivity of the avalanche burial signal and to ensure precise localization through accurate GPS data and efficient data processing. The avalanche transceiver was mounted on the tailboom of the VTOL system - a location with minimal possibility of EMI. The Raspberry Pi serves as the central processing unit (CPU) of the system. The CPU is responsible for managing the Universal Asynchronous Receiver/Transmitter (UART) connection with the avalanche transceiver, which allows real-time data transfer from the transceiver to the central processing

The data received from the avalanche transceiver include the direction and distance of the target, which are used in the subsequent localization algorithms. This data is then merged with the current GPS location and heading information provided by the VTOLsystem. In this state of research, all computationally expensive tasks, such as source localization or visualization, are performed offline on a laptop after the flight. The GPS data are then fused with the distance and direction data from the avalanche transceiver to locate the buried avalanche transceiver. As the current aircraft did not yet have a fully functional autopilot with real-time kinematics (RTK) on board, a HILTI PLT-400 (Hilti, 2025) total station was used to track the target on the ground. The corner points of the search area were obtained with cm-accurate position data.

## 1.4 Target Localization Approach

The magnetic field is generated by a static magnetic dipole based on the analytical formulation shown in 1. A magnetic dipole can be described by its dipole moment **m**. In our case, the dipole moment describes the strength of the dipole and depends on the properties of the coil.

$$\mathbf{B}(r) = \nabla \times \mathbf{A} = \frac{\mu_0}{4\pi} \left[ \frac{3r(\mathbf{m} \cdot r)}{r^5} - \frac{\mathbf{m}}{r^3} \right]$$
(1)

where  $\mathbf{B}(r)$  is the magnetic field generated by the transceiver at distance r,  $\mathbf{m} = (m_x, m_y, m_z)^T$  is the magnetic moment vector of the dipole that is given by the specifications of the avalanche transceivers coils. The constant  $\mu_0$  is the vacuum permeability. In the current state of research, we do not have available  $\mathbf{B}$ 

field data from the avalanche transceiver, but only a distance r and a direction value processed internally. The use of the  $\bf B$  field data would allow us to solve the inverse problem via constrained optimization for a more accurate localization.

We employ a two-stage Extended Kalman Filter (EKF) approach to estimate the (assumed stationary) target coordinates  $(x_{TX}, y_{TX})$ . The first EKF (*Smoothing Filter*) combines the raw directions  $\phi$  and distance r measurements from the avalanche transceiver with GPS position and heading  $(x_{RX}, y_{RX}, h_{RX})$  of the drone for noise reduction. The second EKF (*Tracking Filter*) uses the smoothed measurements to update the target estimate using the non-linear measurement model, shown in 2. In Figure 4 we can find the highlevel schematic of the setup.

$$\begin{cases} x_{RX} + r\cos\phi = x_{TX}, \\ y_{RX} + r\sin\phi = y_{TX}, \end{cases}$$
 (2)

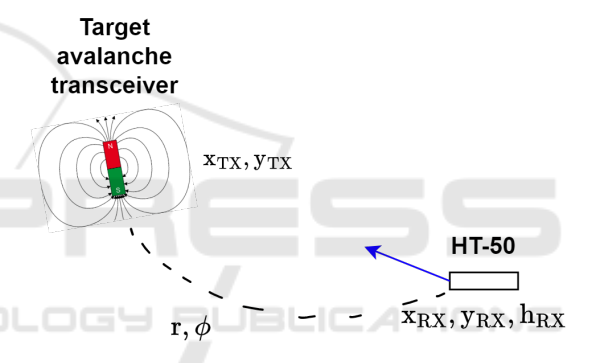


Figure 4: We have used one transceiver device in send mode, as a target. A second system is used in search mode on the VTOL-system to collect data and used for localization.

#### 1.4.1 Smoothing EKF

To robustly fuse coarse avalanche transceiver data with precise GPS position and heading, we implemented a simple EKF that smoothed outliers in direction and distance before propagating a second filter to estimate the absolute location of the target.

## **State and Process Model**

We define the state vector at time k as:

$$\mathbf{x}_k = \begin{bmatrix} \mathbf{\phi}_k \\ r_k \end{bmatrix},\tag{3}$$

where  $\varphi_k$  is the estimated direction to the buried transceiver in degrees, and  $r_k$  is the estimated distance to the target in decimeters. The covariance  $\mathbf{P}_k \in \mathbb{R}^{2 \times 2}$  encodes the uncertainty.

Upon receiving new GPS data, indicating a displacement of  $(\Delta x, \Delta y)$  in meters from successive latitude and longitude readings, we predict the next state. The prediction model, which accounts for the searcher's movement, is given by:

$$\hat{\varphi}_k = \varphi_{k-1} + \alpha \Delta \theta, \tag{4}$$

$$\hat{r}_k = \max(r_{k-1} - \beta \| [\Delta x, \Delta y] \|, r_{\min}), \qquad (5)$$

where:

- $\Delta\theta \in [-180^{\circ}, 180^{\circ}]$  is the angular difference between the GPS-derived motion heading and the previously estimated direction of the transceiver
- $\alpha$  and  $\beta$  are adaptive gain factors that reflect how strongly the searcher's motion is expected to influence the transceiver estimates. These gains are dynamically adjusted on the basis of observed movement.
- $r_{\min} > 0$  is a minimum distance threshold, preventing non-physical negative ranges.

The predicted state covariance matrix  $\hat{\mathbf{P}}_k$  is evolved by adding the process noise covariance matrix  $\mathbf{Q}_k$ :

$$\mathbf{\hat{P}}_k = \mathbf{P}_{k-1} + \mathbf{Q}_{k-1}. \tag{6}$$

The noise of the process  $Q_k$  is dynamically tuned to allow moderate drift in the estimated direction and distance, its magnitude being adjusted based on the speed of the searcher's movement.

## **Measurement Update**

When a new transceiver measurement  $(\varphi_k^{\text{meas}}, r_k^{\text{meas}})$ becomes available, we use a measurement matrix  $\mathbf{H} =$ I, as the measurements directly correspond to the state variables. The residuals (innovations) are formed by comparing the measurement with the predicted state, with a proper angle wrapping in  $[-180^{\circ}, 180^{\circ}]$  for the direction:

$$\mathbf{v}_{\mathbf{o}} = ((\mathbf{o}_{k}^{\text{meas}} - \hat{\mathbf{o}}_{k} + \mathbf{\pi}) \mod 2\mathbf{\pi}) - \mathbf{\pi}, \tag{7}$$

$$y_{\varphi} = ((\varphi_k^{\text{meas}} - \hat{\varphi}_k + \pi) \mod 2\pi) - \pi,$$
 (7)  
 $y_r = r_k^{\text{meas}} - \hat{r}_k.$  (8)

The measurement noise covariance matrix  $\mathbf{R}_k$  is adaptively adjusted based on two primary factors:

• Range-dependent direction noise: A larger measured distance  $r_k^{\text{meas}}$  implies higher directional uncertainty, leading to an increased variance for  $\varphi_k^{\text{meas}}$ .

• Low-motion penalty: If the searcher's movement between updates is minimal ( $\ll 1$  m), both directional and distance variances in  $\mathbf{R}_k$  are scaled up to counteract potential spurious swings or static measurement inaccuracies.

The Kalman gain  $\mathbf{K}_k$  and the subsequent state and covariance updates are calculated as follows:

$$\mathbf{S}_k = \mathbf{H}\mathbf{\hat{P}}_k\mathbf{H}^T + \mathbf{R}_k,\tag{9}$$

$$\mathbf{K}_k = \mathbf{\hat{P}}_k \mathbf{H}^T \mathbf{S}_k^{-1},\tag{10}$$

$$\mathbf{x}_{k} = \begin{bmatrix} \hat{\mathbf{p}}_{k} \\ \hat{r}_{k} \end{bmatrix} + \mathbf{K}_{k} \begin{bmatrix} y_{\mathbf{p}} \\ y_{r} \end{bmatrix}, \tag{11}$$

$$\mathbf{P}_k = (\mathbf{I} - \mathbf{K}_k \mathbf{H}) \,\hat{\mathbf{P}}_k \, (\mathbf{I} - \mathbf{K}_k \mathbf{H})^T + \mathbf{K}_k \mathbf{R}_k \mathbf{K}_k^T. \quad (12)$$

### 1.4.2 Tracking EKF

We employ another Extended Kalman Filter (EKF) to estimate the fixed avalanche transceiver's absolute position  $(x_{TX}, y_{TX})$  in a local Cartesian frame. This filter takes advantage of the smoothed direction and distance measurements provided by the avalanche transceiver.

#### **State and Process Model**

The state vector at time k is defined as the target's estimated position:

$$\mathbf{x}_k = \begin{bmatrix} \mathbf{x}_{\mathrm{TX},k} \\ \mathbf{y}_{\mathrm{TX},k} \end{bmatrix},\tag{13}$$

with its associated covariance matrix  $P_k$  =  $Cov(\mathbf{x}_k)$ . Assuming the target remains stationary, the prediction step simply propagates the state estimate without change.

$$\hat{\mathbf{x}}_k = \mathbf{x}_{k-1}.\tag{14}$$

However, the predicted state covariance evolves by adding a small noise covariance matrix in the process  $\mathbf{Q}_k$ :

$$\hat{\mathbf{P}}_k = \mathbf{P}_{k-1} + \mathbf{Q}_k. \tag{15}$$

The magnitude of  $\mathbf{Q}_k$  is adaptively reduced as the search progresses through its phases (coarse, fine, pinpoint), reflecting an increasing confidence in the target's immobility.

#### Non-linear Measurement Model

At each time step k, the searcher, located at  $(x_{RX}, y_{RX})$  in the same local cartesian frame, obtains smoothed distance  $r_k$  and direction  $\varphi_k$  measurements from the avalanche transceiver. The non-linear measurement function  $h: \mathbb{R}^2 \to \mathbb{R}^2$  relates the target's true position  $(x_{\text{TX}}, y_{\text{TX}})$  to these expected measurements:

$$r_k = \sqrt{(x_{\text{TX}} - x_{\text{RX}})^2 + (y_{\text{TX}} - y_{\text{RX}})^2},$$
 (16)

$$\varphi_k = atan2(y_{TX} - y_{RX}, x_{TX} - x_{RX}).$$
 (1)

Thus, the measurement vector is  $\mathbf{z}_k = [r_k, \, \varphi_k]^{\top}$ .

#### Jacobian Linearization

To incorporate these non-linear measurements into the EKF framework, the measurement function h is linearized about the predicted state  $\hat{\mathbf{x}}_k$ . This yields the measurement Jacobian matrix  $\mathbf{H}_k$ :

$$\mathbf{H}_{k} = \frac{\partial h}{\partial \mathbf{x}} \bigg|_{\hat{\mathbf{x}}_{k}} = \begin{bmatrix} \frac{x_{\mathrm{TX}} - x_{\mathrm{RX}}}{\hat{r}_{k}} & \frac{y_{\mathrm{TX}} - y_{\mathrm{RX}}}{\hat{r}_{k}} \\ -\frac{y_{\mathrm{TX}} - y_{\mathrm{RX}}}{\hat{r}_{k}^{2}} & \frac{x_{\mathrm{TX}} - x_{\mathrm{RX}}}{\hat{r}_{k}^{2}} \end{bmatrix}, \quad (18)$$

where  $\hat{r}_k$  is the predicted smoothed distance calculated using the predicted state  $\hat{\mathbf{x}}_k$  and the searcher's position  $(x_{RX}, y_{RX})$ . To avoid singularities when the searcher is very close to the estimated target position, for very small  $\hat{r}_k$  (specifically,  $\hat{r}_k < 0.01$  m), we substitute  $\mathbf{H}_k \approx \mathbf{I}$ .

#### Measurement Noise Adaptation

The measurement noise covariance matrix  $\mathbf{R}_k$  is defined as:

$$\mathbf{R}_k = \begin{bmatrix} \mathbf{\sigma}_r^2 & 0\\ 0 & \mathbf{\sigma}_{\mathbf{\phi}}^2 \end{bmatrix},\tag{19}$$

where:

- $\sigma_r$  is the standard deviation of the distance measurement. Scales with the measured range  $r_k$  (e.g.  $\sigma_d \approx 0.1 r_k$  in phase 1, with a minimum of 1 meter) and is significantly reduced in later search phases (fine, pinpoint).
- $\sigma_{\phi}$  is the standard deviation of the direction measurement. It is also distance-dependent (inversely proportional to range) and is further inflated if the searcher is receding from the target. The variances for both distance and direction are dynamically adjusted based on the current search phase, with higher confidence assigned to measurements received during later phases.

#### **Update Equations**

The innovation vector (residual)  $\mathbf{y}_k$  is formed by comparing the actual measurement  $\mathbf{z}_k$  with the predicted measurement  $h(\hat{\mathbf{x}}_k)$ , ensuring proper angular wrapping for the direction component:

$$\mathbf{y}_k = \begin{bmatrix} r_k - \hat{r}_k \\ (\varphi_k - \hat{\varphi}_k + \pi) \mod 2\pi - \pi \end{bmatrix}.$$
 (20)

Here,  $\hat{r}_k$  and  $\hat{\varphi}_k$  are the predicted distance and direction based on  $\hat{\mathbf{x}}_k$ .

The subsequent EKF update equations are applied:

$$\mathbf{S}_k = \mathbf{H}_k \, \hat{\mathbf{P}}_k \, \mathbf{H}_k^\top + \mathbf{R}_k, \tag{21}$$

$$\mathbf{K}_k = \hat{\mathbf{P}}_k \mathbf{H}_k^{\top} \mathbf{S}_k^{-1}, \tag{22}$$

$$\mathbf{x}_k = \hat{\mathbf{x}}_k + \mathbf{K}_k \, \mathbf{y}_k,\tag{23}$$

$$\mathbf{P}_k = (\mathbf{I} - \mathbf{K}_k \mathbf{H}_k) \hat{\mathbf{P}}_k (\mathbf{I} - \mathbf{K}_k \mathbf{H}_k)^T + \mathbf{K}_k \mathbf{R}_k \mathbf{K}_k^T.$$
(24)

The Kalman gain  $\mathbf{K}_k$  is further modulated based on the search phase and whether the searcher is approaching or receding from the target.

# 2 RESULTS

The performance of the proposed VTOL-based localization approach was evaluated in an open field test site of about  $50m \times 50m$ . We adopted a horizontal sweep search pattern as described in (Blankenship et al., 2022), varying the spacing between the lines, the flight height and the flight speed of the helicopter. In total, ten flights were executed, not all on the same day and on the same location.

The helicopter was manually controlled by an experienced pilot, who was informed of current altitude above ground (AGL) and current flight speed at regular intervals from another operator reading out flight information from a ground station terminal.

# 2.1 Ground Tests

Prior to flight tests, we performed stationary ground tests to assess the impact of sensor placement on the sensitivity of localization during turbine running. By mounting the avalanche transceiver on the VTOL tailboom, thus increasing distance from the gas turbine, fuel pump and onboard electronics, we improved the effective detection range from approximately 10 m to up to 30 m. This threefold gain demonstrates that simple mechanical separation from high-EMI components can markedly enhance transceiver signal quality.

## 2.2 Sensitivity Experiments

As an initial test, the sensitivity of the sensor system was analyzed during flying. For this purpose, the target was placed with an offset of 3 m in the x and y directions to the helicopter. The VTOL system then flew vertically upward during data recording. The results in Figure 5 showed that it is possible to track the

target up to a distance of 30 m. Compared to the tests by (Ricciardi, 2017), we achieved a range that was three to four times higher.

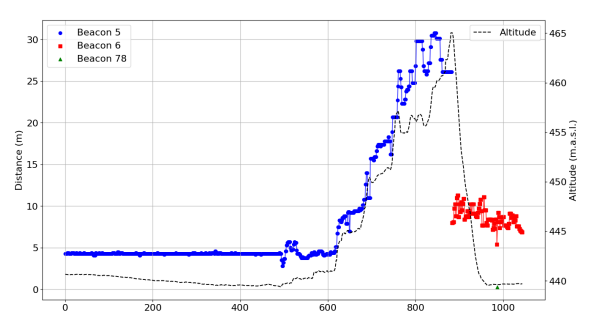


Figure 5: The collected distance data from the transceiver to the target is shown in blue. The dashed black line shows the height of the VTOL system in meters above sea level (m.a.s.l.). After the system had reached an altitude of 30 m, the helicopter turned off and then began tracking another target (shown in red and green), but this is not relevant to the test result.

# 2.3 Test-Flight Experiments

Following ground validation and sensitivity analysis, we conducted in total ten flights to investigate the limits of the system.

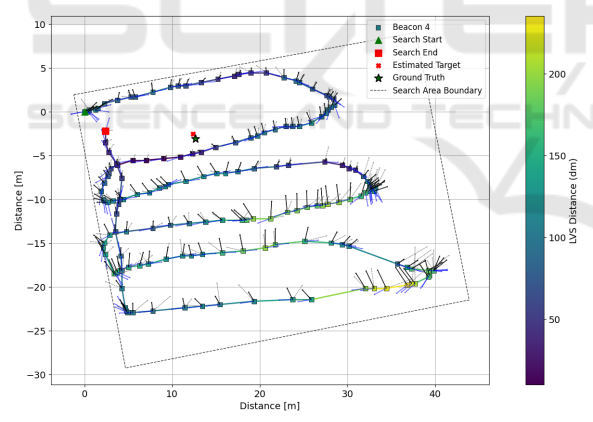


Figure 6: Results of a test-flight: raw transceiver direction (dotted gray arrows) and distance (colored markers), current transceiver ID (markers shape), smoothed direction and position (black arrows), and final estimated target location (red cross) and ground truth (green star). The dotted line around the flight path marks the search area boundary.

For the test flight in Figure 6 we chose a spacing between the lines of 5 m. The pilot flew at a height of 3 m above ground and a speed of 2 m/s. Both, altitude and airspeed, varied slightly due to the lack of an autopilot. The green and red squares show the start and stop points of the helicopter.

# 2.4 Flight-Path and Target Localization

The direction readings (dotted gray arrows) and distance measurements (colored markers) in Figure 6are the noisy raw data collected from the avalanche transceiver. After smoothing the direction and distance, the estimated target location (red cross) converges near the true target location (green star). The Euclidean distance between the ground truth and the estimation was 0.63,m in this experiment. Using RTK positioning of the drone could further increase the localization accuracy.

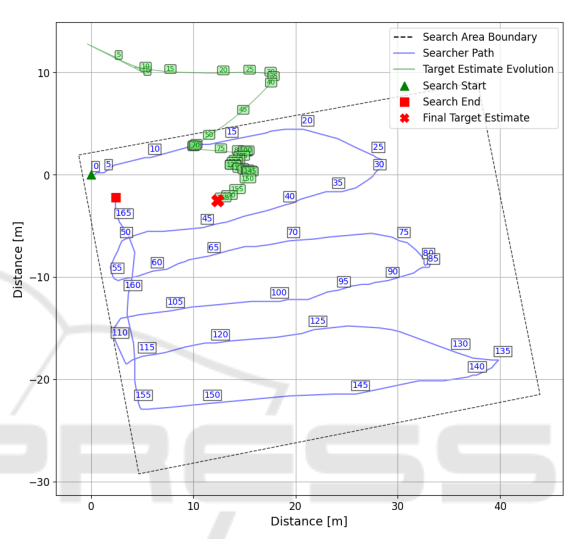


Figure 7: Evolution of the Tracking EKF's estimated target position (in green) in the horizontal plane over time. The blue lines show the flight path. The numbers indicates the current index of the datapoint.

Figure 7 depicts the Tracking EKF's state estimate of the target's  $(x_{TX}, y_{TX})$  coordinates. The plot shows how the position of the target estimated by the EKF converges in the proximity of the ground truth position.

## 2.5 Discussion

The purpose of the paper was to demonstrate the functionality of a helicopter-based localization system. The current state-of-the-art is and remains companion rescue.

The added value of the system comes into play in dangerous conditions or in very large avalanche cones, where it is difficult to move on foot. Field tests must be carried out to compare such scenarios, but this has not yet been done and will only be the case when the system is further developed.

# 3 CONCLUSION

In this work, we have presented a novel VTOL-based avalanche victim localization system that overcomes key limitations of existing brushless motor-driven platforms presented in section 1.2. By replacing noisy DC motors with a turbine, we effectively avoided EMI issues in avalanche transceiver signals and demonstrated submeter localization accuracy under realistic field conditions. The use of a turbine-powered VTOL system allows operations in cold weather conditions and rugged alpine terrain, greatly extending the practical utility of search and rescue missions.

In the future, we plan to integrate raw **B** field vector measurements directly from the avalanche transceiver coil to refine position estimates and improve the overall localization precision. We will also explore inverse optimization methods to enable simultaneous tracking of multiple buried subjects. To realize a fully end-to-end rescue solution, future work will focus on:

- Developing (semi-) autonomous flight trajectories for rapid deployment to the accident site,
- Incorporating on-board camera and LiDAR sensors for real-time estimation of the avalanche cone geometry and safe landing zones,
- Designing a reliable target-marking mechanism such as visual markers to guide ground teams to located victims.

These advances will be critical to the delivery of a complete and life-saving system capable of autonomous search, pinpoint location, and target marking in harsh mountain environments.

## **ACKNOWLEDGEMENTS**

The authors appreciate the support provided by GPV AG and MAMMUT AG. Their provision of avalanche transceivers, as well as the corresponding interfaces and communication protocols, was essential for the development and execution of this research. The authors also thank HILTI AG for providing the PLT 400 total station and support with data extraction. The project was funded by Innosuisse's Innovation Booster Robotics program.

## REFERENCES

Alcedo (2010). Alcedo: A drone-based avalanche rescue prototype. Unpublished student project report, ETH Zurich.

- ANAVIA (2025a). Ht-100. ANAVIA (2025b). Ht-50.
- Association, A. A. (2025). Avalanche fatalities statistics. https://avalanches.org/fatalities/fatalities-statistics/. [Accessed: April 23, 2025].
- ATLASUAS (2025). Atlasavalanche pro system overview. Product brochure; employs a flexible transceiver mounting to reduce EMI.
- Ayuso, N., Cuchí, J., Lera, F., and Villarroel, J. (2015). A deep insight into avalanche transceivers for optimizing rescue. *Cold Regions Science and Technology*, 111:80–94.
- Azzollini, I. A., Mimmo, N., Gentilini, L., and Marconi, L. (2020). Uav-based search and rescue in avalanches using arva: An extremum seeking approach. In *IFAC-PapersOnLine*, volume 53, pages 1627–1632.
- Blankenship, R., Bluman, J., and Steckenrider, J. (2022). An investigation of search algorithms for aerial reconnaissance of an area target. In *Proceedings of the Annual General Donald R. Keith Memorial Conference*, pages 72–77, West Point, New York, USA. IEWorld-Conference.org. A Regional Conference of the Society for Industrial and Systems Engineering.
- Bluebird (2021). Powderbee drone system. Dissolved on August 10, 2021.
- Brugger, H., Etter, H. J., Zweifel, B., Mair, P., Hohlrieder, M., Ellerton, J., Elsensohn, F., Boyd, J., Sumann, G., and Falk, M. (2007). The impact of avalanche rescue devices on survival. *Resuscitation*, 75(3):476–483.
- DJI (2025). Matrice 200 series.
- ETSI (2017). Avalanche beacons operating at 457 khz; transmitter–receiver systems; part 1: Harmonised standard for access to radio spectrum.
- Falk, M., Brugger, H., and Adler-Kastner, L. (1994). Avalanche survival chances. *Nature*, 368(6466):21–21.
- Hilti (2025). Plt 400-4 digitale absteckgeräte. https://www.hilti.ch/content/hilti/CH/de/home.html. Laser measuring tool.
- Janovec, M., Kandera, B., and Šajbanová, K. (2022). Using unmanned aerial vehicles during the search of people buried in an avalanche. *Transportation Research Pro*cedia, 65:350–360.
- Mammut (2024a). Barryvox pulse. Older generation summit beacon, discontinued 2017.
- Mammut (2024b). Barryvox s. Avalanche transceiver with 3-antenna digital/analog, 70 m search strip width.
- Nivitec (2020). Nivitec drone assisted avalanche rescue system. project inactive since 2020.
- Ricciardi, F. (2017). Automatic Search of Missing People in Avalanches. Master's thesis, Alma Mater Studiorum – University of Bologna, Bologna, Italy.
- Silvagni, M., Tonoli, A., Zenerino, E., and Chiaberge, M. (2017). Multipurpose uav for search and rescue operations in mountain avalanche events. *Geomatics, Natural Hazards and Risk*, 8(1):18–33.
- Toson, F., De Giudici, F., Piva, A., and Menegatti, E. (2021). Averla: Autonomous drone for avalanche rescue. In *Proceedings of the XXVI AIDAA Congress*.